

# 2 GIS – based groundwater potentiality mapping using AHP 3 and FR models in central Antalya, Turkey

4  
5 Hemayatullah Ahmadi<sup>1,3\*</sup>, Ozumcan Alara Kaya<sup>1</sup>, Ebru Babadagi<sup>1</sup>, Turan Savas<sup>2</sup>, Emrah Pekkan<sup>1,2</sup>  
6

7 <sup>1</sup> Department of Remote Sensing and Geographic Information System, Graduate School of Sciences, Eskisehir Technical  
8 University, Eskisehir, Turkey

9 <sup>2</sup> Institute of Earth & Space Sciences Eskisehir, Technical University, Eskisehir, Turkey

10 <sup>3</sup> Department of Geological Engineering and Exploration of Mines, Kabul Polytechnic University, Faculty of Geology and  
11 Mining, Kabul, Afghanistan

12 \* Correspondence: [h.ahmadi@kpu.edu.af](mailto:h.ahmadi@kpu.edu.af) / [hahmadi@eskisehir.edu.tr](mailto:hahmadi@eskisehir.edu.tr) ; Tel.: +90-552-266-4876

13 **Abstract:** Groundwater is considered as one of the essential natural resources stored beneath the earth surface by  
14 infiltration through various rock layers. Groundwater potential supplies almost 30% of fresh water in the world,  
15 and in general, 65% of groundwater is used for agricultural irrigation, 25% as drinking water, and the remaining  
16 10% is utilized as industrial water. The main aim of this study is to delineate groundwater potential zones in the  
17 central Antalya province, Turkey using the analytical hierarchy process (AHP) and frequency ratio (FR). Seven  
18 thematic layers including lithology, slope, drainage density, landcover/landuse, lineament density, rainfall, and  
19 soil depth were considered as influencing parameters to run these models. The preparation of all geospatial  
20 datasets was carried out in GIS environment and Google Earth Engine. Besides, some authorized relevant web  
21 portals were also tried for obtaining the required spatial data. The findings of analysis by AHP and FR models  
22 show that Muratpasa, Kepez, and eastern Dosemealti in the eastern part of study area are characterized by high  
23 potentiality of groundwater, while the regions in southern, western parts covered by igneous rocks and other less  
24 permeable sediments, also featured by high and steep slopes are followed by low or very low groundwater  
25 potential. Consequently, the results from both models were assessed using receiver operating curve (ROC) and  
26 area under curve (AUC) for validation. The validation in this study confirms the higher effectivity of results  
27 achieved by FR than the AHP model.

28 **Keywords:** GIS, groundwater, AHP, FR, potential, lithology  
29

## 30 1. Introduction

31 Groundwater is considered as one of the vital elements of nature which is found in the voids of the earth and  
32 packs the pore space of soil beneath the water table [1–4]. Groundwater is proven as one of the most significant  
33 natural resources which is dependent as a source of water supply in all climatic regions of the world [5, 6]. Almost  
34 30% of the world's fresh water is supplied by groundwater while only 0.3% is furnished by surface water  
35 including lakes, reservoirs, and rivers [4, 7]. The main sources of groundwater are rainwater and snowmelt which  
36 are leaching down through the soil pores into the aquifer [8].

37 At present time due to rapid growth of industrialization and population, demands on fresh water directly  
38 affected on groundwater has been increasing which is a worldwide concern, therefore exploitation of  
39 groundwater is considered as an essential part of water management and planning [4, 7]. The availability of  
40 groundwater resources depends on the diverse geological, morphological, biological and atmospheric  
41 characteristics factors including lithology, topographic condition, geologic structures, climate, soil type and many

42 other, and the movement mainly depends on the porosity, permeability, transmissibility, and the storage capacity  
43 of the rocks [9–12].

44 There are several approaches for targeting groundwater potential by considering these factors. The  
45 applicable methods are geological, geophysical and remote sensing which have been examined by many  
46 scientists. The efficiency of methods are varied, some of them are more effective, accurate, time saving and with  
47 less cost, while the traditional methods are time consuming and require high expenses [13–15]. Furthermore,  
48 integration of GIS and remote sensing studies has the capability to analyse and store huge amounts of geospatial  
49 data and delineate groundwater potential using different methods [4, 15, 16].

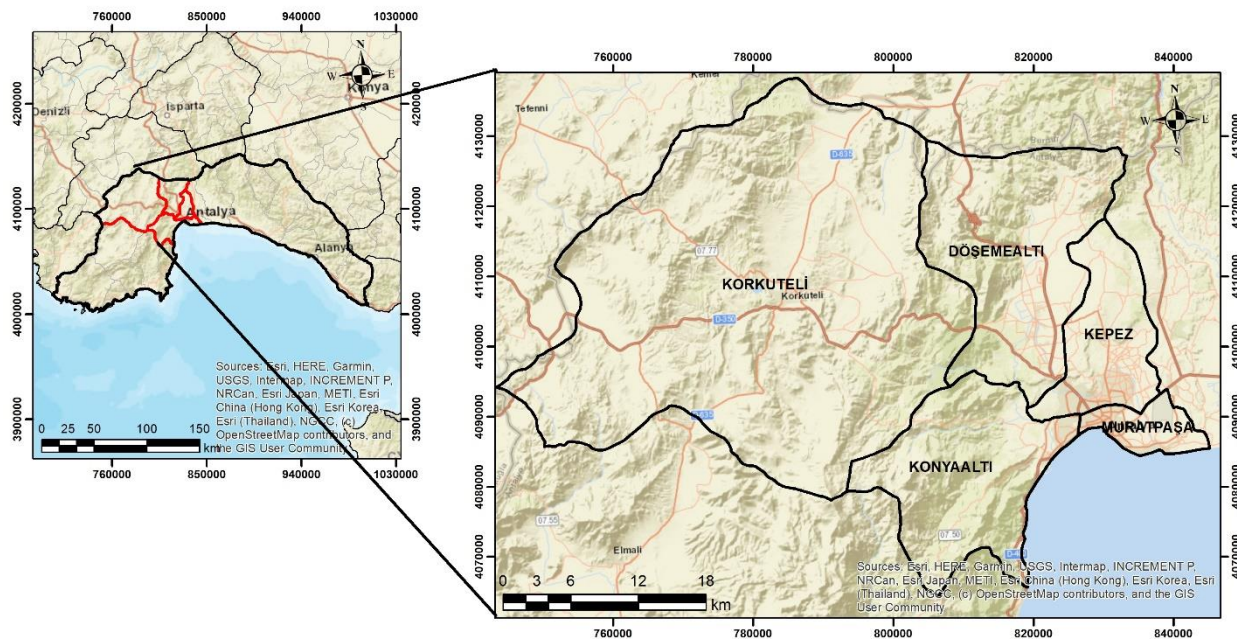
50 Several studies have been carried out for groundwater management using various multi-criterial decision  
51 making and learning machines algorithms [12, 13, 17–19]. Diverse studies have been undertaken on groundwater  
52 potential mapping using Analytical Hierarchy Process (AHP), Frequency Ratio (FR), and Influencing Factor [4,  
53 15, 20–26]. Some other researchers have examined logistic model tree, Dempster-Shafer model, certainty factor,  
54 logistic regression, random forest model, maximum entropy model, decision tree model, artificial neural network  
55 for delineation of groundwater potentiality [27–31].

56 Central Antalya is mostly covered by agricultural areas consuming groundwater reservoirs, also in some  
57 areas, groundwater is characterized by pollutants. Due to Mediterranean climate, the study area is characterized  
58 by hot and dry weather in summer and warm weather in winter, hence distinct groundwater management and  
59 planning is required to overcome the problems arising from drought. The initial planning is highlighting  
60 groundwater potential mapping. Therefore, this study aims to delineate the groundwater potential zones using  
61 AHP and FR models in a GIS environment. The findings of this study sufficiently contribute to further detailed  
62 groundwater related studies, agricultural irrigation planning, urban planning in Antalya province. Central  
63 Antalya is mostly covered by agricultural areas consuming groundwater reservoirs, also in some areas,  
64 groundwater is characterized by pollutants. Due to Mediterranean climate, the study area is characterized by hot  
65 and dry weather in summer and warm weather in winter, hence distinct groundwater management and planning  
66 is required to overcome the problems arising from drought. The initial planning is highlighting groundwater  
67 potential mapping. Therefore, this study aims to delineate the groundwater potential zones using AHP and FR  
68 models in a GIS environment. The findings of this study sufficiently contribute to further detailed groundwater  
69 related studies, agricultural irrigation planning, urban planning in Antalya province.

70  
71

## 72 **2. Study area**

73 Central Antalya is located in the south western part of Turkey within the 29°44' - 35°52' longitudes and  
74 36°41' - 37°20' latitudes over the Antalya Travertine Plateau. It contains the area of almost 4060 km<sup>2</sup> which  
75 covers the 5 districts; Korkuteli, Dosemealti, Kepez, Muratpasa, and Konyaalti. Regionally the study area is  
76 bordered with Sparta, Burdur, Denizli provinces and Toros Mountains in the the north and with the  
77 Mediterranean sea in the south east (Figure 1). The study area is characterized by Mediterranean climate which  
78 is hot and dry in summer and warm – rainy in winter seasons.



79

80 Figure 1. Location of study area

81

82 **3. Material and Methods**

83 Geographic Information System and remote sensing were used in this study to map groundwater potential  
 84 zones by examining analytical hierarchy process and frequency ratio models. Totally seven thematic layers  
 85 including lithology, slope, drainage density, landcover/landuse, lineament density, rainfall, and soil depth were  
 86 generated and weighted considering the expert ideas and previous literature. The whole design of methodology  
 87 is depicted in (Figure 2).

88

89 **3.1. Generation of Geospatial Datasets**

90 Remotely sensed, conventional, and climatic data were provided from different organizations and  
 91 authorized websites to generate thematic layers influencing groundwater potential. Lithology of an area is the  
 92 most critical factor while considering groundwater potential zones, as rock porosity and permeability have direct  
 93 impact on groundwater movement and availability [4, 15, 32]. The lithological map of the study area in scale  
 94 1:25000 was extracted from the geological map of Turkey prepared by the General Directorate of Mineral Research  
 95 and Exploration (MTA) of Turkey. The map was processed and reclassified for analysis using ArcGIS 10.5 (Figure  
 96 3A). Considering the influence of geology on groundwater potential, most of the study area is covered by  
 97 sedimentary and metamorphic rocks, as one of the largest travertine plateaus of Turkey is situated in the eastern  
 98 part including Kepez, Muratpasa, and south eastern part of Dosemealti districts. Moreover, central, western, and  
 99 northern parts of the study area are covered by alluvium and sandstone formation which are good indicators of  
 100 groundwater recharge. Based on the presence of igneous rocks within the south east and south west, it is judged  
 101 that groundwater activities are less in these areas due to less permeability of rocks.

102 Several studies describe that slope and drainage density have significant roles in run off and penetration of  
 103 water which control the groundwater. SRTM DEM was downloaded from the USGS website through scripting in  
 104 Google Earth Engine and was processed in GIS environment. Both slope and drainage density thematic layers  
 105 were classified into five classes. The areas with high slope pave the way for high runoff and erosion and less  
 106 permeability, while the areas with gentle slope correspond to less runoff and high infiltration [15, 23, 33] (Figure  
 107 3B). It is seen that Kepez, Muratpasa, eastern Dosemealti, and central Korkuteli districts within the study area  
 108 comprise gentle slopes (0 – 16 o), while the western part of Dosemealti, and most of Konyaalti districts are  
 109 characterized by moderate slopes of (32 – 48 o), only 3% of the study area accounts for steep slope (54 – 80o).

110 Drainage density has also significant influence on run off and groundwater infiltration as the high density  
 111 of drainage indicates high runoff and less groundwater recharge whereas high groundwater infiltration and less

runoff are characterized by less drainage density [4, 34, 35]. The drainage network of the study area was prepared and analyzed for density using ArcGIS, the resultant map was classified and resampled into five classes (Figure 3C). It is considered that drainage density within the study area is ranging between (0 – 2.87 km<sup>-1</sup>) corresponding to moderate interval. The classes of drainage density have almost equal distribution over the area except the last class which has limited extension.

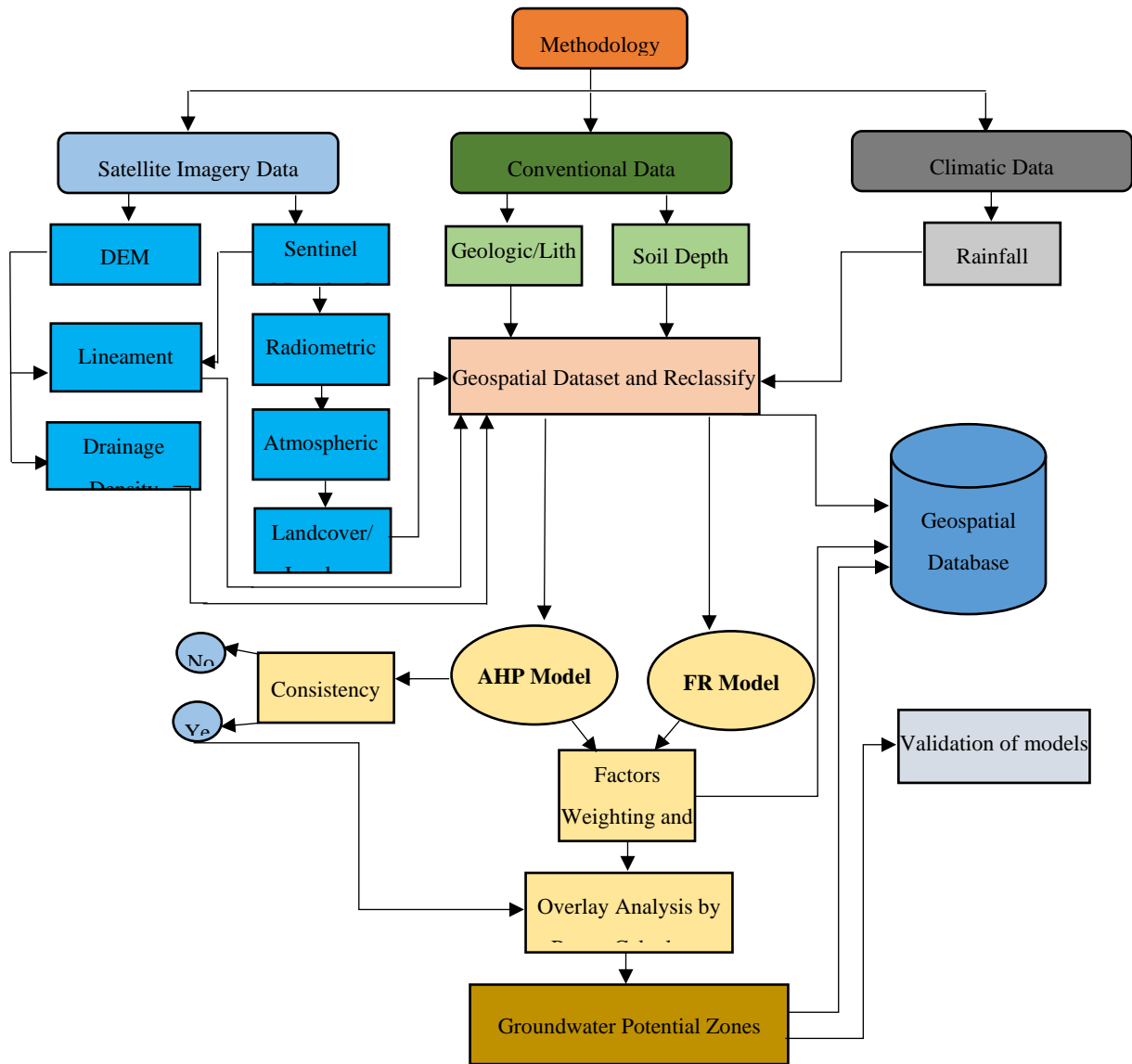


Figure 2. Flowchart describing the methodology

Land pattern and coverage play an essential role for development of groundwater activities as land covered by vegetation, forest and greening influence high infiltration of groundwater, while land covered by builtup areas decrease recharge and increase runoff flow. In this study, the landcover/landuse map was prepared by integration of Sentinel 2 MSI and CORINE Land Cover 2018 from the official website of Copernicus. The classification was carried out in Google Earth Engine, ENVI 5.7, and ArcGIS 10.5. The final landcover/landuse map is characterized by 9 classes: forest, sparse plants, natural grassland, agricultural areas, urban areas, mining extraction areas, waterbodies, bare soil, and bare rocks (Figure 3D). It declares that most of the area is covered by forests and agricultural areas, and limited sections in the south eastern part are dedicated to build up areas. The water body reservoirs have limited distribution over the study area. The forests, agricultural areas, grasslands, and sparse plants significantly help the process of groundwater activities and recharge.

Lineaments are defined as linear or curvilinear structures on the earth surface and are indicators of weaker zones of bed rocks. Lineament density has a fundamental role in groundwater potential indirectly as the high potential zones of groundwater are followed by high density of lineaments [23]. The lineament map was prepared using visual interpretation and automatic extraction in this study. SRTM DEM 30m and Landsat 8 were used to automatically extract lineaments using ArcGIS and PCI Geomatica software. Visual interpretation and elimination of all anthropogenic features such as roads, canals, rivers, etc. were conducted on the resultant map to achieve the final thematic layer. The final map was targeted to generate the lineament density map processed in the GIS environment (Figure 3E). The existence of lineaments on igneous rocks are effective for groundwater recharge, however in this study, lineaments with high density are found farther from igneous masses. The lineaments trend in NE-SW direction.

The rainfall factor is considered as one of the most significant hydrologic elements which crucially effect groundwater recharge [15, 36]. Rainfall data was downloaded from the official web portal of Center for Hydrometeorology and Remote Sensing (CHRS) with spatial resolution of 1km for 10 years between 2009 to 2020. An average annual rainfall map for the study area was generated and resampled as raster data in ArcGIS Desktop (Figure 3F). The rainfall map shows that coastal areas experience less annual precipitation than eastern and central parts. Rainfall is one of the main sources of groundwater within the study area which ranges between 401.42 – 549 mm annually.

Soil depth is another important control on groundwater potential as a region with higher depth of soil is a place for developing of higher potential of groundwater. The soil depth spatial map was prepared using well log data in GIS environment (Figure 3G). South western and northern parts are characterized by deep soil depth, whereas central and western parts have shallow and moderate soil coverage.

### 3.2. Analytical Hierarchy Process (AHP)

AHP is a multicriteria model for complex decision making through assessing multiple factors which was first introduced by [37]. The model stands for inputting influencing parameters which are accomplished by the opinions and knowledge of experts [15, 38]. Based on [39], the AHP model contains the definition of objectives, determination of required criteria, pairwise comparisons and matrices preparation, determining relative weights using eigenvalue techniques, calculating consistency ratio of model, and final decision-making steps.

The influence and importance of each factor are defined by making a pairwise matrix and the factors are valued on [37] scale from 1 (equal significance) to 9 (extreme significance) shown in (Table 1).

Table1. Pairwise comparison matrix between all factors for AHP model

Factors	Factors						
	Lithology	Slope	Drainage Density	Landcover/Landuse	Lineament Density	Rainfall	Soil Depth
Lithology	1.00	3.00	4.00	5.00	5.00	7.00	6.00
Slope	1/3	1.00	2.00	2.00	4.00	5.00	6.00
Drainage Density	1/4	½	1.00	2.00	3.00	4.00	5.00
Landcover/Landuse	1/5	½	1/2	1.00	2.00	3.00	4.00
Lineament Density	1/5	¼	1/3	1/2	1.00	2.00	3.00
Rainfall	1/7	1/5	1/4	1/3	1/2	1.00	1.00
Soil Depth	1/6	1/6	1/5	1/4	1/3	1.00	1.00
<i>Sum</i>	2.29	5.61	8.28	11.08	15.83	23.00	26.00

163 The normalized pairwise comparison matrix is prepared by division of each cell by the total of each column,  
 164 normalized weights are obtained for each factor by the average of each row shown in (Table 2).  
 165

166 Table 2. Normalized pairwise comparison matrix and weights of each factor

Factors	Factors							Weights
	Lithology	Slope	Drainage Density	Landcover/ Landuse	Lineament Density	Rainfall	Soil Depth	
Lithology	0.4361	0.5341	0.4829	0.4511	0.3158	0.3043	0.2308	0.3936
Slope	0.1454	0.1780	0.2414	0.1805	0.2526	0.2174	0.2308	0.2066
Drainage Density	0.1090	0.0890	0.1207	0.1805	0.1895	0.1739	0.1923	0.1507
Landcover/Landuse	0.0872	0.0890	0.0604	0.0902	0.1263	0.1304	0.1538	0.1054
Lineament Density	0.0872	0.0445	0.0402	0.0451	0.0632	0.0870	0.1154	0.0689
Rainfall	0.0623	0.0356	0.0302	0.0301	0.0316	0.0435	0.0385	0.0388
Soil Depth	0.0727	0.0297	0.0241	0.0226	0.0211	0.0435	0.0385	0.0360
<i>Sum</i>	1.0000	1.0000	1.0000	1.0000	1.0000	1.0000	1.0000	1.0000

167

168 Once the weights are assigned, it is required to calculate consistency of the matrix, it is judged by the  
 169 Consistency Ratio following equation developed by [37].

170 
$$CR = \frac{CI}{RI}$$

171 Where, CR is consistency ratio, CI is consistency index, RI is random index which is taken from a table  
 172 prepared by [37]. It depends on the number of criteria and in this study, it is equal to 1.32. CI is calculated using  
 173 the following equation:

174 
$$CI = \frac{\lambda_{max} - n}{n - 1}$$

175 Where,  $\lambda_{max}$  is the principle eigenvalue of the matrix and is calculated from the matrix that comes to 7.3 in  
 176 this study, n is the number of factors considered for groundwater potential which is 7. According to [37, 40], the  
 177 CR obtained must be less than 0.1. If it comes greater than 0.1, then the pairwise comparison matrix should be  
 178 readjusted by assigning different values to factors [41]. The CR of this study was found  $0.0342 < 0.1$  which judges  
 179 the consistency of matrix.

180 All the factors were classified into sub classes and were ranked based on their impact on groundwater  
 181 activities. Finally the ranks of each sub class were normalized by division of each rank value into summation of  
 182 all ranks as shown in (Table 3).

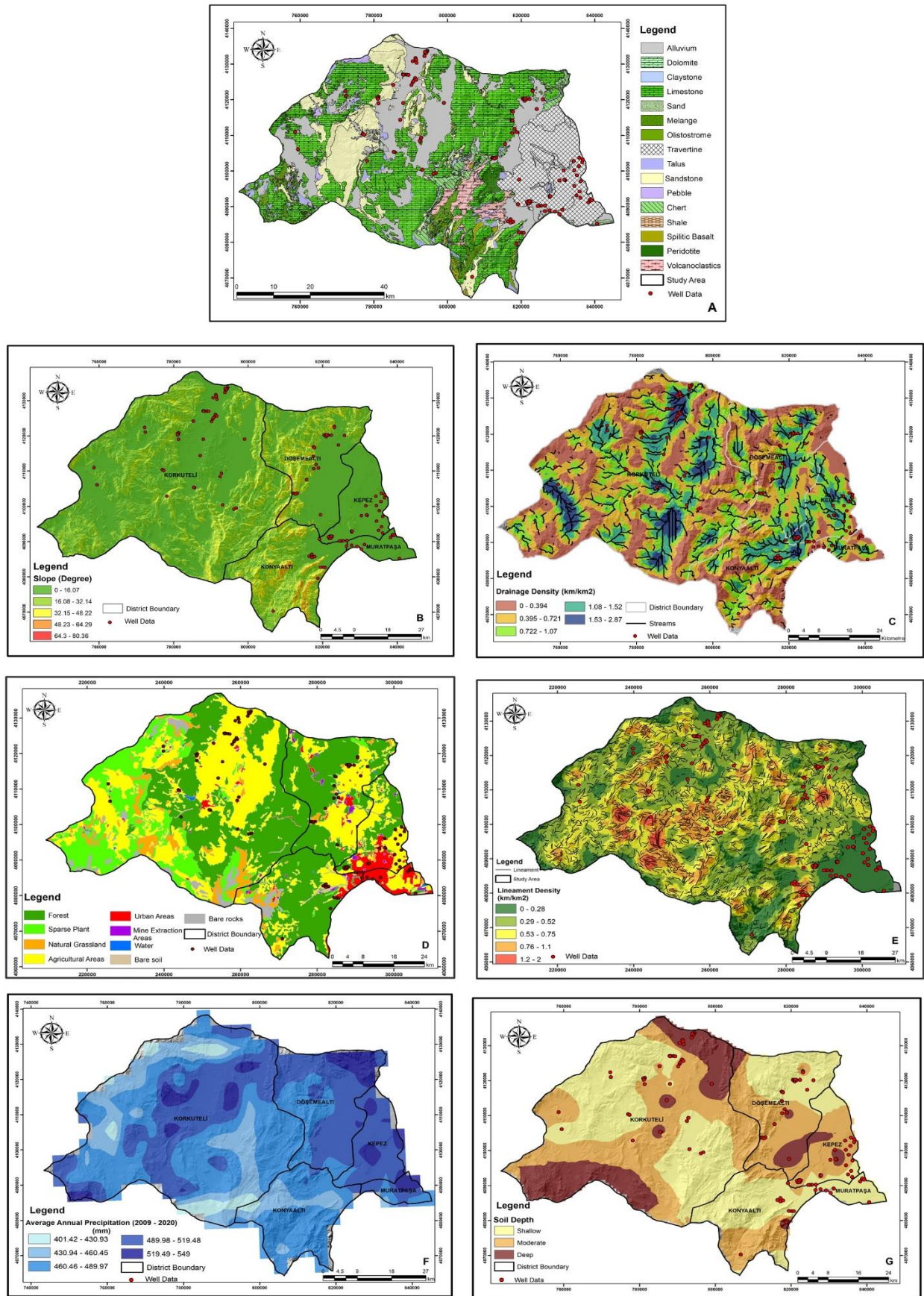
183 The groundwater potential zones (GPZ) were obtained by application of the following equation carried out  
 184 through raster calculator or ArcGIS.

185

186 
$$GPZ = \sum_{i=1}^n AHP = Lt_W Lt_R + Sl_W Sl_R + DD_W DD_R + LC/LU_W LC/LU_R + LD_W LD_R + Rf_W Rf_R + SD_W SD_R$$

187 Where, GPZ is groundwater potential zone, AHP is Analytical Hierarchy Process, Lt is lithology, Sl is slop,  
 188 DD is drainage density, LC/LU is landcover/landuse, LD is lineament density, Rf is rainfall, SD is soil depth, W  
 189 is weighting, and R is rating.





190

191

192

Table 3. Assigned normalized weights and rates for all factors and sub – classes

No	Factors	Sub – Classes	Rating	Normalized Rates	Weights
1	Lithology	Alluvium	6	0.113	0.3936
		Dolomite	3	0.057	
		Claystone	1	0.019	
		Limestone	7	0.132	
		Sand	4	0.075	
		Melange	2	0.038	
		Olistostrome	2	0.038	
		Travertine	6	0.113	
		Talus	2	0.038	
		Sandstone	4	0.075	
		Pebble	3	0.057	
		Chert	6	0.113	
		Shale	1	0.019	
		Spilitic Basalt	2	0.038	
		Peridotite	2	0.038	
2	Slope	Volkanoclastics	2	0.038	0.2066
		< 16.07	5	0.333	
		16.08 – 32.14	4	0.267	
		32.15 – 48.22	3	0.200	
		48.23 – 64.29	2	0.133	
3	Drainage Density	> 64.3	1	0.067	0.1507
		< 0.394	5	0.333	
		0.395 – 0.721	4	0.267	
		0.722 – 1.07	3	0.200	
		1.08 – 1.52	2	0.133	
4	Landcover/Landuse	> 1.53	1	0.067	0.1054
		Bare Rocks	2	0.050	
		Mine Extraction areas	3	0.075	
		Natural Grasslands	4	0.100	
		Forests	7	0.175	
		Sparse Plants	5	0.125	
		Waterbodies	8	0.200	
		Agricultural areas	5	0.125	
		Bare soil	4	0.100	
		Urban areas	2	0.050	
5	Lineament Density	< 0.28	1	0.067	0.0689
		0.29 – 0.52	2	0.133	
		0.53 – 0.75	3	0.200	
		0.76 – 1.1	4	0.267	



		> 1.1	5	0.333	
		< 430.93	1	0.067	
6	Rainfall	430.94 – 460.45	2	0.133	0.0388
		460.46 – 489.97	3	0.200	
		489.98 – 519.48	4	0.267	
		> 519.49	5	0.333	
		Shallow	2	0.200	
7	Soil Depth	Moderate	3	0.300	0.0360
		Deep	5	0.500	

194

195 **3.3. Frequency Ratio (FR)**

196 Frequency ratio is a bivariate statistical model applied as an essential tool for geospatial assessment to  
 197 determine the probabilistic relationship between dependent and independent variables or multi classified  
 198 thematic layers [11, 15]. [42] asserted that FR is considered as the probability of occurrence of a certain factor. In  
 199 groundwater potential mapping, it is applied based on the relationship between distribution of observational  
 200 wells and parameters influencing groundwater potential [4]. Frequency ratio in this study was calculated using  
 201 the following equation:

202

$$FR = \left[ \frac{\left( \frac{P_{gw}}{T_{gw}} \right)}{\left( \frac{P_f}{T_f} \right)} \right] = \frac{\% \text{ wells}}{\% \text{ pixels}}$$

203

204 Where, FR stands for frequency ratio, P\_gw is the number of pixels with groundwater well for each sub class  
 205 of a factor, T\_gw is total number of wells, P\_f is the number of pixels in each sub class of a factor, T\_f is the total  
 206 number of pixels of a factor. In this study, a total of 141 well data with high yield were used, and the FR was  
 calculated by the integration of FR of each sub class of factors in ArcGIS 10.5 using the following formula:

207

$$GPZ = \sum_{i=1}^n FR = Lt_{FR} + Sl_{FR} + DD_{FR} + LC/LU_{FR} + LD_{FR} + Rf_{FR} + SD_{FR}$$

208

209 Where, GPZ is the groundwater potential zone, FR is frequency ratio. The data considered in the above  
 formula was calculated in Table 4.

210

211 Table 4. Spatial relationship between factors and wells with assigned FR for each sub-class

No	Factors	Sub – Classes	No of pixels	Percentage of sub class	No of wells	Percentage of wells	FR
1	Lithology	Alluvium	345076	21.25	69	48.94	2.303
		Dolomite	1028	0.06	0	0.00	0.000
		Claystone	2737	0.17	0	0.00	0.000
		Limestone	592052	36.46	12	8.51	0.233
		Sand	3532	0.22	3	2.13	9.783

		Melange	49510	3.05	0	0.00	0.000
		Olistostrome	16588	1.02	0	0.00	0.000
		Travertine	211013	12.99	48	34.04	2.620
		Talus	45655	2.81	1	0.71	0.252
		Sandstone	220921	13.60	7	4.96	0.365
		Pebble	11176	0.69	0	0.00	0.000
		Chert	52394	3.23	1	0.71	0.220
		Shale	234	0.01	0	0.00	0.000
		Spilitic Basalt	9309	0.57	0	0.00	0.000
		Peridotite	15059	0.93	0	0.00	0.000
		Volkanoclastics	47714	2.94	0	0.00	0.000
		< 16.07	662532	40.80	111	78.72	1.930
2	Slope	16.08 – 32.14	391247	24.09	16	11.35	0.471
		32.15 – 48.22	319286	19.66	4	2.84	0.144
		48.23 – 64.29	197243	12.15	7	4.96	0.409
		> 64.3	53571	3.30	3	2.13	0.645
3	Drainage Density	< 0.394	401889	24.84	17	12.06	0.485
		0.395 – 0.721	483391	29.87	25	17.73	0.593
		0.722 – 1.07	394551	24.38	33	23.40	0.960
		1.08 – 1.52	256027	15.82	41	29.08	1.838
		> 1.53	82206	5.08	25	17.73	3.490
		Bare Rocks	35418	2.18	0	0.00	0.000
		Mine Extraction areas	9376	0.58	0	0.00	0.000
4	Landcover/Land use	Natural Grasslands	82159	5.06	8	5.67	1.121
		Forests	668037	41.17	29	20.57	0.500
		Sparse Plants	219736	13.54	3	2.13	0.157
		Waterbodies	3168	0.20	0	0.00	0.000
		Agricultural areas	535478	33.00	70	49.65	1.504
		Bare soil	5256	0.32	0	0.00	0.000
		Urban areas	63977	3.94	31	21.99	5.576
5	Lineament Density	< 0.28	59630	14.71	51	36.17	2.460
		0.29 – 0.52	111176	27.42	35	24.82	0.905
		0.53 – 0.75	123274	30.40	37	26.24	0.863
		0.76 – 1.1	83001	20.47	10	7.09	0.346
		> 1.1	28416	7.01	8	5.67	0.810
6	Rainfall	< 430.93	53933	3.28	6	4.26	1.298
		430.94 – 460.45	234155	14.24	9	6.38	0.448
		460.46 – 489.97	674202	40.99	46	32.62	0.796
		489.98 – 519.48	566163	34.42	65	46.10	1.339
		> 519.49	116440	7.08	15	10.64	1.503

		Shallow	717956	44.23	72	51.06	1.155
7	Soil Depth	Moderate	648620	39.96	47	33.33	0.834
		Deep	256656	15.81	22	15.60	0.987

212

213 **4. Results and Discussion**

214 Considering the 7 most influential thematic layers on groundwater potential, the map deduced from AHP and FR  
 215 calculation was prepared and classified into four classes based on the Jenk classification scheme in ArcGIS 10.5 ranging  
 216 from very low, low, and moderate to high classes.

217 For AHP analysis which is a common multi criteria decision maker model for various geospatial investigation, all the  
 218 considered thematic layers were classified differently, while most of them are into five classes. The factors, and sub – classes  
 219 were weighted and ranked based on their importance and having the opinions of relevant experts. The overall CR was  
 220 obtained 0.034 which show the high consistency of model application. The resultant map by AHP model (Figure 4a) shows  
 221 that 24% and 39% of the total area of central Antalya province is characterized by moderate and high groundwater potential  
 222 (Table 5). These areas have almost regular distribution over all the districts except for Konyalti. The land coverage shows  
 223 that areas covered by travertine, alluvium and agricultural sites having moderate and high groundwater potential.

224 The very low and low potential are seen over areas covered by less greening or igneous rocks. Frequency ratio (FR) was  
 225 applied to find the ratio between the percentage of wells availability within a certain class and area of each sub class of a  
 226 factor [15]. As described in (Table 4), higher FR is found for sand sediments in which the lithology factor is 9.783.

227 In the slope factor, flat areas are followed about 79% of all well, hence the slope less than 16 degree is having the highest  
 228 FR which is (1.93). In this study, the frequency ratio is getting high by increasing the drainage density as a density of more  
 229 than 1.53 km-1 accounts for the highest FR of (3.49). The same trending of ratios is seen in other case studies as well by [4,  
 230 15]. Considering the landcover pattern, the higher number of wells are seen within agricultural and urban areas, which show  
 231 the highest frequency ratios of 1.5 and 5.57. The largest number of wells are distributed within the lesser density of lineaments  
 232 hence they have the highest FR of 2.46. The regions highlighted by the highest amount of annual precipitation are  
 233 characterized by highest frequency ratio (1.5). Almost 50% of groundwater wells were drilled within the regions with shallow  
 234 thickness of soil, therefore they have higher FR (1.15). The final resultant map by FR model was also classified into four  
 235 classes according to Jenk Classification Scheme and showing that 48% of the study area is characterized by low and moderate  
 236 groundwater potential while only 4% of the region contains high potential (Figure 4b..) (Table 5).

237

238

239

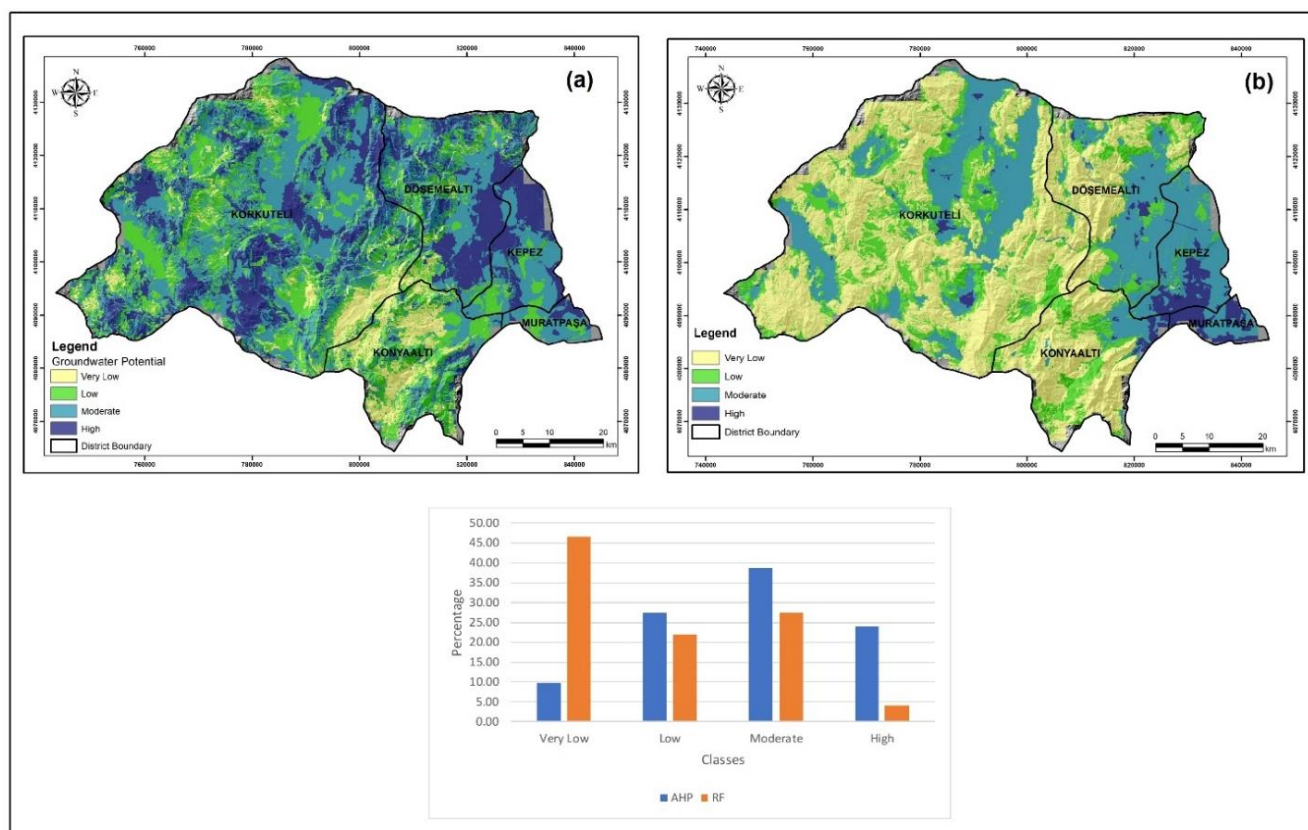
Table 5. The distribution of groundwater potential classes based on AHP and FR models.

Class	AHP Model			FR Model		
	Range	Area (km2)	Area (%)	Range	Area (km2)	Area (%)
Very Low	0.0743 – 0.1472	377.125	9.71	2.4140 – 5.6005	1807.733	46.54
Low	0.1473 – 0.1717	1068.54	27.51	5.6006 – 8.6277	853.6725	21.98
Moderate	0.1718 – 0.1922	1508.575	38.84	8.6278 – 12.7702	1066.238	27.45
High	0.1923 – 0.243	930.17	23.95	12.7703 – 22.7280	156.8275	4.04

240

241

242



243

244

Figure 4. The groundwater potential maps for central Antalya, Turkey by a) AHP Model, b) FR Model.

245

#### 246 4.1. Validation

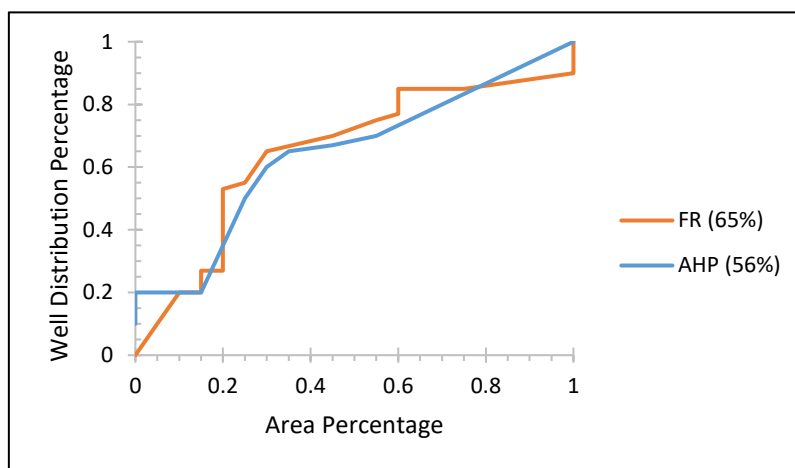
247

248 Each model must be validated as [43] asserts that a model finds its significance when it is validated. There are several  
 249 methods for checking the accuracy and validation of groundwater potential maps generated by AHP and FR models. The  
 250 most usable validation techniques are receiver operating characteristics (ROC) analysis and area under curve (AUC) which have  
 251 been examined by several scholars [4, 6, 15, 20, 44]. In this study wells with high yield and a generated groundwater potential  
 252 dataset were considered to analyse the ROC curve. The ROC curve was prepared by considering the percentage of  
 253 groundwater potential classes on the x axis and percentage of groundwater wells on the y axis.

254

255 Once the ROC was created, AUC was calculated to find the accuracy of models and the correct occurrence or non-  
 256 occurrence of pre-defined classes (Figure 5). The quantitative – qualitative of AUC for the AHP model was calculated 0.56  
 257 (or accuracy of 56%), while AUC for FR model shows 0.65 (accuracy of 65%). Based on [15, 45], the AUC values  
 258 corresponding to prediction accuracy can be divided into: poor (0.5 – 0.6), average (0.6 – 0.7), good (0.7 – 0.8), very good  
 259 (0.8, 0.9), and excellent(0.9 – 1). Calculation and plotting of AUC for both models shows that results from FR model are  
 more efficient than AHP model in the study area.

259



260  
261  
262  
263  
264

Figure 5. Chart showing the ROC curve and AUC for AHP and FR models

265 **5. Conclusions**

266 Groundwater potential mapping has been carried out using different traditional and remotely based approaches for  
267 decades. The use of remote sensing technology and GIS makes it easy and accessible for experts to conduct potential mapping  
268 with low effective costs and time consumed. Various spatial and non-spatial modelling using GIS environment are applied  
269 to demarcate groundwater potential in which their accuracy is different. In this study, analytical hierarchy process and  
270 frequency ratio models were applied by considering seven thematic layers: lithology, slope, drainage density,  
271 landcover/landuse, lineament density, rainfall, and soil depth.

272 By giving high importance to lithology of the region and less importance to the soil depth layer, Muratpasa, Kepez, and  
273 eastern Dosemealti districts are followed by the high potential of groundwater based on both models. The main reasons for  
274 high potential of these districts are existence of a huge travertine plateau which makes an environment for higher permeability  
275 of groundwater. The regions are characterized by steep slopes, also igneous rocks coverage is directed to low and very low  
276 groundwater potential due to huge amounts of run off on the surface. The regions covered by agricultural, forest areas and  
277 alluvium have moderate potential for groundwater.

278 The reliability of the AHP model for groundwater potential demarcation is directly dependent on the assignment of the  
279 weights and ranks to each class and sub-class. Therefore, deep study and knowledge on factors influencing the targeted object  
280 are required, also the geographical, geological, and hydrological characteristics of the study area are another point to be  
281 contemplated. Implementation of FR does not require more knowledge of users to set ranks or weights, while the model itself  
282 finds ratio of factors which gives more reliable results. The final resultants maps and validation confirm that groundwater  
283 potential mapped by FR is more reliable and efficient than the AHP model. The results from this study can be a hint for the  
284 responsible departments to have accurate future planning of groundwater in terms of distribution, planning, consumption,  
285 and artificial recharge. Moreover, the findings should be followed with further detailed field work and other relevant studies  
286 to accomplish accurate groundwater potential mapping at large scale over the small districts and villages.

287  
288 **Conflict of interest**

289 The authors declare that there is not any potential conflict arising out of this paper. The paper is also not accompanied  
290 by any funding resources.

291 **References**

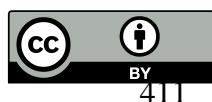
292 1. Fitts C (2002) Groundwater science  
293 2. Bagyaraj M, Ramkumar T, Venkatramanan S, Gurugnanam B (2013) Application of remote sensing and  
294 GIS analysis for identifying groundwater potential zone in parts of Kodaikanal Taluk, South India. Front  
295 Earth Sci 7:65–75. <https://doi.org/10.1007/s11707-012-0347-6>



- 296 3. Naghibi SA, Pourghasemi HR, Pourtaghi ZS, Rezaei A (2015) Groundwater qanat potential mapping using  
297 frequency ratio and Shannon's entropy models in the Moghan watershed, Iran. *Earth Sci Informatics*  
298 8:171–186. <https://doi.org/10.1007/s12145-014-0145-7>
- 299 4. Das S (2019) Comparison among influencing factor, frequency ratio, and analytical hierarchy process  
300 techniques for groundwater potential zonation in Vaitarna basin, Maharashtra, India. *Groundw Sustain*  
301 *Dev* 8:617–629. <https://doi.org/10.1016/j.gsd.2019.03.003>
- 302 5. Todd D, Mays L (2004) *Groundwater hydrology*
- 303 6. Manap MA, Sulaiman WNA, Ramli MF, et al (2013) A knowledge-driven GIS modeling technique for  
304 groundwater potential mapping at the Upper Langat Basin, Malaysia. *Arab J Geosci* 6:1621–1637.  
305 <https://doi.org/10.1007/s12517-011-0469-2>
- 306 7. Senanayake IP, Dissanayake DMDOK, Mayadunna BB, Weerasekera WL (2016) An approach to delineate  
307 groundwater recharge potential sites in Ambalantota, Sri Lanka using GIS techniques. *Geosci Front* 7:115–  
308 124. <https://doi.org/10.1016/j.gsf.2015.03.002>
- 309 8. Banks D, Robins N (2002) *An introduction to Groundwater in Crystalline Bedrock*
- 310 9. Mukherjee S (1996) Targeting saline aquifer by remote sensing and geophysical methods in a part of  
311 Hamirpur-Kanpur, India. *Hydrogeol J* 19:53–64
- 312 10. Ganapuram S, Kumar GTV, Krishna IVM, et al (2009) Mapping of groundwater potential zones in the  
313 Musi basin using remote sensing data and GIS. *Adv Eng Softw* 40:506–518.  
314 <https://doi.org/10.1016/j.advengsoft.2008.10.001>
- 315 11. Oh HJ, Kim YS, Choi JK, et al (2011) GIS mapping of regional probabilistic groundwater potential in the  
316 area of Pohang City, Korea. *J Hydrol* 399:158–172. <https://doi.org/10.1016/j.jhydrol.2010.12.027>
- 317 12. Das S, Pardeshi SD (2018) Integration of different influencing factors in GIS to delineate groundwater  
318 potential areas using IF and FR techniques: a study of Pravara basin, Maharashtra, India. *Appl Water Sci*  
319 8:. <https://doi.org/10.1007/s13201-018-0848-x>
- 320 13. Jha MK, Chowdary VM, Chowdhury A (2010) Groundwater assessment in Salboni Block, West Bengal  
321 (India) using remote sensing, geographical information system and multi-criteria decision analysis  
322 techniques. *Hydrogeol J* 18:1713–1728. <https://doi.org/10.1007/s10040-010-0631-z>
- 323 14. Nampak H, Pradhan B, Manap MA (2014) Application of GIS based data driven evidential belief function  
324 model to predict groundwater potential zonation. *J Hydrol* 513:283–300.  
325 <https://doi.org/10.1016/j.jhydrol.2014.02.053>
- 326 15. Razandi Y, Pourghasemi HR, Neisani NS, Rahmati O (2015) Application of analytical hierarchy process,  
327 frequency ratio, and certainty factor models for groundwater potential mapping using GIS. *Earth Sci*  
328 *Informatics* 8:867–883. <https://doi.org/10.1007/s12145-015-0220-8>
- 329 16. Al-Shabeeb AAR, Al-Adamat R, Al-Fugara A, et al (2018) Delineating groundwater potential zones within  
330 the Azraq Basin of Central Jordan using multi-criteria GIS analysis. *Groundw Sustain Dev* 7:82–90.  
331 <https://doi.org/10.1016/j.gsd.2018.03.011>
- 332 17. Jasrotia AS, Kumar R, Saraf AK, et al (2007) *International Journal of Remote Sensing* Delineation of  
333 groundwater recharge sites using integrated remote sensing and GIS in Jammu district, India Delineation  
334 of groundwater recharge sites using integrated remote sensing and GIS in Jammu district, India. *Taylor*  
335 *Fr* 28:5019–5036. <https://doi.org/10.1080/01431160701264276>
- 336 18. Magesh NS, Chandrasekar N, Soundranayagam JP (2012) Delineation of groundwater potential zones in  
337 Theni district, Tamil Nadu, using remote sensing, GIS and MIF techniques. *Geosci Front* 3:189–196.  
338 <https://doi.org/10.1016/j.gsf.2011.10.007>

- 339 19. Naghibi SA, Moradi Dashtpajardi M (2017) Evaluation of four supervised learning methods for  
340 groundwater spring potential mapping in Khalkhal region (Iran) using GIS-based features. *Hydrogeol J*  
341 25:169–189. <https://doi.org/10.1007/s10040-016-1466-z>
- 342 20. Ozdemir A (2011) GIS-based groundwater spring potential mapping in the Sultan Mountains (Konya,  
343 Turkey) using frequency ratio, weights of evidence and logistic regression methods and their comparison.  
344 *J Hydrol* 411:290–308. <https://doi.org/10.1016/j.jhydrol.2011.10.010>
- 345 21. Sener E, Davraz A (2013) Assessment of groundwater vulnerability based on a modified DRASTIC model,  
346 GIS and an analytic hierarchy process (AHP) method: The case of Egirdir Lake basin (Isparta, Turkey).  
347 *Hydrogeol J* 21:701–714. <https://doi.org/10.1007/s10040-012-0947-y>
- 348 22. Rahmati O, Nazari Samani A, Mahdavi M, et al (2015) Groundwater potential mapping at Kurdistan  
349 region of Iran using analytic hierarchy process and GIS. *Arab J Geosci* 8:7059–7071.  
350 <https://doi.org/10.1007/s12517-014-1668-4>
- 351 23. Hossein A, Ardakani H, Ekhtesasi MR (2016) Groundwater potentiality through Analytic Hierarchy  
352 Process (AHP) using remote sensing and Geographic Information System (GIS)
- 353 24. Jenifer MA, Jha MK (2017) Comparison of Analytic Hierarchy Process, Catastrophe and Entropy  
354 techniques for evaluating groundwater prospect of hard-rock aquifer systems. *J Hydrol* 548:605–624.  
355 <https://doi.org/10.1016/j.jhydrol.2017.03.023>
- 356 25. Guru B, Seshan K, Bera S (2017) Frequency ratio model for groundwater potential mapping and its  
357 sustainable management in cold desert, India. *J. King Saud Univ. - Sci.* 29:333–347
- 358 26. Şener E, Şener Ş, Davraz A (2018) Groundwater potential mapping by combining fuzzy-analytic hierarchy  
359 process and GIS in Beyşehir Lake Basin, Turkey. *Arab J Geosci* 11:. [https://doi.org/10.1007/s12517-018-](https://doi.org/10.1007/s12517-018-3510-x)  
360 [3510-x](https://doi.org/10.1007/s12517-018-3510-x)
- 361 27. Mogaji KA, Lim HS, Abdullah K (2015) Regional prediction of groundwater potential mapping in a  
362 multifaceted geology terrain using GIS-based Dempster–Shafer model. *Arab J Geosci* 8:3235–3258.  
363 <https://doi.org/10.1007/s12517-014-1391-1>
- 364 28. Naghibi SA, Pourghasemi HR, Dixon B (2016) GIS-based groundwater potential mapping using boosted  
365 regression tree, classification and regression tree, and random forest machine learning models in Iran.  
366 *Environ Monit Assess* 188:1–27. <https://doi.org/10.1007/s10661-015-5049-6>
- 367 29. Zabihi M, Pourghasemi HR, Pourtaghi ZS, Behzadfar M (2016) GIS-based multivariate adaptive regression  
368 spline and random forest models for groundwater potential mapping in Iran. *Environ Earth Sci* 75:.  
369 <https://doi.org/10.1007/s12665-016-5424-9>
- 370 30. Chen W, Li H, Hou E, et al (2018) GIS-based groundwater potential analysis using novel ensemble  
371 weights-of-evidence with logistic regression and functional tree models. *Sci Total Environ* 634:853–867.  
372 <https://doi.org/10.1016/j.scitotenv.2018.04.055>
- 373 31. Lee S, Hong SM, Jung HS (2018) GIS-based groundwater potential mapping using artificial neural network  
374 and support vector machine models: the case of Boryeong city in Korea. *Geocarto Int* 33:847–861.  
375 <https://doi.org/10.1080/10106049.2017.1303091>
- 376 32. Golkarian A, Rahmati O (2018) Use of a maximum entropy model to identify the key factors that influence  
377 groundwater availability on the Gonabad Plain, Iran. *Environ Earth Sci* 77:.  
378 [https://doi.org/10.1007/s12665-](https://doi.org/10.1007/s12665-018-7551-y)  
[018-7551-y](https://doi.org/10.1007/s12665-018-7551-y)
- 379 33. Prasad RK, Mondal NC, Banerjee P, et al (2008) Deciphering potential groundwater zone in hard rock  
380 through the application of GIS. *Environ Geol* 55:467–475. <https://doi.org/10.1007/s00254-007-0992-3>
- 381 34. Dinesh Kumar PK, Gopinath G, Seralathan P (2007) *International Journal of Remote Sensing Application*

- 382 of remote sensing and GIS for the demarcation of groundwater potential zones of a river basin in Kerala,  
383 southwest coast of India Application of remote sensing and GIS for the demarcation of groundwater . Int  
384 J Remote Sens 28:5583–5601. <https://doi.org/10.1080/01431160601086050>
- 385 35. Saha D, Dhar Y, assessment SV-E monitoring and, 2010 undefined (2010) Delineation of groundwater  
386 development potential zones in parts of marginal Ganga Alluvial Plain in South Bihar, Eastern India.  
387 Springer 165:179–191. <https://doi.org/10.1007/s10661-009-0937-2>
- 388 36. Adiat KAN, Nawawi MNM, Abdullah K (2012) Assessing the accuracy of GIS-based elementary multi  
389 criteria decision analysis as a spatial prediction tool - A case of predicting potential zones of sustainable  
390 groundwater resources. J Hydrol 440–441:75–89. <https://doi.org/10.1016/j.jhydrol.2012.03.028>
- 391 37. Saaty T (1990) Decision making for leaders: the analytic hierarchy process for decisions in a complex world
- 392 38. Kumar A, Krishna AP (2018) Assessment of groundwater potential zones in coal mining impacted hard-  
393 rock terrain of India by integrating geospatial and analytic hierarchy process (AHP) approach. Geocarto  
394 Int 33:105–129. <https://doi.org/10.1080/10106049.2016.1232314>
- 395 39. Hosseinali F, Alesheikh AA (2008) Weighting spatial information in GIS for copper mining exploration.  
396 Am J Appl Sci 5:1187–1198. <https://doi.org/10.3844/ajassp.2008.1187.1198>
- 397 40. Malczewski J (1999) GIS and multicriteria decision analysis
- 398 41. Saaty TL (1977) A scaling method for priorities in hierarchical structures. J Math Psychol 15:234–281.  
399 [https://doi.org/10.1016/0022-2496\(77\)90033-5](https://doi.org/10.1016/0022-2496(77)90033-5)
- 400 42. Bonham-Carter, F G (1994) Geographic information systems for geoscientists: Modelling with GIS.  
401 Comput methods Geosci 13:398. [https://doi.org/10.1016/0098-3004\(95\)90019-5](https://doi.org/10.1016/0098-3004(95)90019-5)
- 402 43. Fabbri A, Chung C-JF, Fabbri AG (2003) Validation of Spatial Prediction Models for Landslide Hazard  
403 Mapping. Nat Hazards 30:451–472. <https://doi.org/10.1023/B:NHAZ.0000007172.62651.2b>
- 404 44. Andualem TG, Demeke GG (2019) Groundwater potential assessment using GIS and remote sensing: A  
405 case study of Guna tana landscape, upper blue Nile Basin, Ethiopia. J Hydrol Reg Stud 24:  
406 <https://doi.org/10.1016/j.ejrh.2019.100610>
- 407 45. Yesilnacar E (2005) The application of computational intelligence to landslide susceptibility mapping in  
408 Turkey. Univ Melbourne, PhD Thesis



© 2020 by the authors; licensee MDPI, Basel, Switzerland. This article is an open access article distributed under the terms and conditions of the Creative Commons by Attribution (CC-BY) license (<http://creativecommons.org/licenses/by/4.0/>).